Linear response theory for two neural populations applied to gamma oscillation generation

Alexandre Payeur,[1] Jérémie Lefebvre,[2] Leonard Maler,[3] and André Longtin[1]

[1]*Department of Physics, University of Ottawa, 150 Louis-Pasteur, Ottawa, Canada K1N 6N5*

[2]*Department of Neuroscience, University of Geneva, CMU-1 Rue Michel-Servet, Geneva, Switzerland, 1211 Geneva 4*

[3]*Department of Cell and Molecular Medicine, University of Ottawa, 451 Smyth Rd., Ottawa, Canada K1H 8M5*

Linear response theory (LRT) can be used to compute spectral properties of single and populations of stochastic leaky integrate-and-fire neurons. The effects of inputs, both external and from delayed feedback, can be modeled within that theory when the neural function is sufficiently linearized by noise. It has been used to explain experiments where gamma oscillations are induced by spatially correlated stochastic inputs to a network with delayed inhibitory feedback. Here we expand this theory to include two distinct population types. We first show how to deal with homogeneous networks where both types of neurons have identical intrinsic properties. We further tackle the asymmetric case, where noise or bias differ. We also analyze the case where the membrane time constants differ, based on experimental evidence, which requires delicate alterations of the theory. We directly apply the theory to networks of ON and OFF cells in the electrosensory system, which together provide global delayed negative feedback to all cells; however, ON and OFF cells receive external inputs of opposite polarities. Theoretical results are in excellent agreement with numerical simulations of the two population network. In contrast to the case of a single ON cell population with feedback, the more realistic presence of both cell types can significantly reduce the propensity of the delayed feedback network to oscillate for spatially correlated inputs. Our results are further linked to recent predictions from deterministic neural field theory. Among other findings, our work suggests that the observed gamma oscillations could be explained only if the ON and OFF cell feedback pathways are anatomically segregated. Thus our two population LRT can make specific predictions about network topography in specific systems.

I. INTRODUCTION

Collective oscillations are common in neural assemblies [1,2]. Mechanisms by which neurons are able to fire rhythmically in more or less synchronized patterns have been explored at the cellular and network levels [3]. A general question is how interactions, both recurrent and with external inputs, determine the properties of coherent oscillations. A well-known type of neural rhythm is gamma oscillations, which occur in the frequency band 30–90 Hz; their exact functions remain elusive [4]. The nonlinear character of nerve cells and the noisy environments in which they evolve often complicate the analysis of population dynamics. However, intrinsic noise may linearize the single-neuron behavior with respect to external inputs and allow useful approximations [5]. Here, such an approach—backed by numerical simulations—will be taken to study gamma oscillations in neural nets involved in the electrosense of weakly electric fish.

Weakly electric fish—and other creatures as well—must be able to ascertain the nature of a given stimulus, be it a prey, a predator, a conspecific, or a pattern in their habitat, so that their behavioral response is appropriate. Stimuli differ by their physical properties and dimensions and, as a corollary, by the topology and timing of the signals they send to the electrosensory lateral lobe line (ELL), the first-order processing center of electrosensory stimuli (see [6] for a review). The pyramidal cells of the ELL receive inputs from cutaneous electroreceptors, which sense the amplitude of the electric field surrounding their body. Thus, a prey will excite a small area of their body (local stimulus), whereas a signal from a conspecific will stimulate a large proportion of the electroreceptors (global signal). A global signal may be either spatially correlated (e.g., communication signals from conspecifics), uncorrelated (e.g., large irregular rocks), or anything in between. We assume that a spatially correlated global signal stimulates concurrently all the electroreceptors.

A first step in the sensory discrimination process may be achieved through shifts of the dominant oscillation frequency of the sensory network. By dominant oscillation frequency, we have in mind the frequency at which the power spectrum of the cells' spike train reaches a local maximum. It is established that the ELL pyramidal cells will enter an oscillatory state when submitted to globally extended random signals [7–9]. These oscillations are in the gamma range with a dominant frequency ≈50 Hz and seem to involve a synchronous activity of the cells [7]. Less clear is the effect of a local or a spatially uncorrelated global stimulus, both seemingly eliciting weak low-frequency oscillations (≈15–20 Hz), with the spikes being largely uncorrelated [7–9].

The ELL cells are subdivided into two classes depending on their response to excitatory inputs: ON cells (or E cells) increase their firing rate, whereas OFF cells (I cells) decrease their firing rate with respect to their baseline activities. Almost every OFF cell is adjacent to an ON cell [10] and both share a common receptive field center. The network studied in this paper may be viewed as a one-dimensional layer of ON and OFF cell pairs receiving inputs from the skin. The ELL's pyramidal cells are mainly connected through a feedback loop, not by direct synaptic connections [11]. Delayed feedback is a potent mechanism by which network activity may oscillate. In the case of ELL pyramidal cells, a delayed inhibitory feedback is responsible for the onset of oscillations [7].

Networks of leaky integrate-and-fire (LIF) neurons of the ON type—connected via delayed inhibitory feedback and receiving external Gaussian noise—were used to model the ELL circuitry [7,9,12,13]. The neural population responsible for the feedback signal together with the excitatory ON cells, form an excitatory-inhibitory network. These networks are fertile breeding grounds for gamma oscillations [4]. Using linear response theory (LRT), Refs. [9,12] and particularly [13], have explained that gamma oscillations arise in the ELL due to the interplay between a correlated input and the delayed feedback. However, OFF cells were completely ignored in these works. Henceforth, this type of network, where OFF cells are absent, will be called ON-only networks. On the other hand, neural field studies of ON and OFF cell (ON/OFF) networks [14,15] showed that the latter are less likely to exhibit rhythmic activity compared to ON-only networks under constant, spatially localized inputs.

In this paper, we derive a LRT for the ON/OFF network and use it to analyze the impact of the OFF cells on the network oscillations. In the symmetric case, for which the properties of the ON and OFF cells are identical except for the way they receive inputs, we find that the OFF cells impede the oscillations found in the ON-only network. This extends some conclusions of [14,15] to stochastic stimuli. We then try to break that symmetry based on physiological knowledge, to see if we can recover the gamma oscillations. It appears that oscillations can be brought back, but not at an intensity comparable to that of either the ON-only network [13] or the experimental results of [9]. This suggests that the ON and OFF cells belong to segregated pathways, i.e., ON (OFF) cells are connected dominantly through feedback to ON (OFF) cells.

The paper is structured as follows: First, we present the model in detail. Then, we use the LRT to write the perturbed spike trains in terms of the unperturbed activity plus a small quantity. This allows us to obtain approximate analytical expressions for the spectral quantities. For this, we based ourselves heavily on [13]. The analytical results must then be adapted to Gaussian white noise inputs of unlimited bandwidth, which will be the external stimuli used for most of this paper to allow comparison with [13]. We then present the results of numerical simulations together with the LRT for the various cases mentioned in the preceding paragraph. For the symmetric case, we compare the behavior of the ON-only and the ON/OFF networks. The symmetry between the ON and OFF cells is first broken by changing the bias and the intensity of the internal noise of OFF cells. Also we change the time scale over which the OFF cells evolve with respect to the ON cells, together with an increase of the OFF cells' bias. Beyond the context of electric fish, our results illustrate how LRT can be applied to nonhomogeneous neural nets.

II. MODEL

We consider a network of $2N$ LIF neurons distributed into N ON/OFF pairs, as illustrated in Fig. 1. The relevant dynamical variables are the subthreshold membrane potentials and the quantities of interest are the spike trains for each neuron. The LIF scheme prescribes that a spike occurs whenever a given threshold V_T is reached by a membrane potential V. After a refractory time, the membrane potential
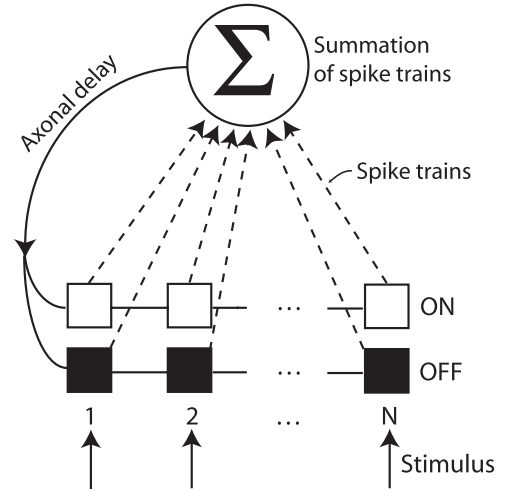

FIG. 1. Schema of the network. Both ON and OFF cells receive external stimuli. Whenever the firing threshold is reached, a spike is fired. A remote kernel sums the spike trains and feeds them back to the network with a delay in an all-to-all fashion.

is reset to a potential V_R. The dynamics of the subthreshold potentials are of the form

$$C_m \dot{V} = -g_L(V - E_L) + \text{noise},$$

with C_m the membrane capacitance, g_L the leak conductance, and E_L the reversal potential. In what follows, we will use nondimensionalized versions of the equation above [13]. Namely, we define the bias current μ and the potential v:

$$\mu \equiv \frac{E_L - V_R}{V_T - V_R}, \quad v \equiv \frac{V - V_R}{V_T - V_R}. \tag{1}$$

With this rescaling, the threshold becomes $v_T = 1$, the reset $v_R = 0$, and time is measured in units of the membrane constant C_m/g_L, which is supposed to be the same for ON and OFF cells for now. The refractory time will be denoted by τ_R.

In the absence of any inputs and feedback, the subthreshold spontaneous activities of the ON and OFF neurons are given by

$$\begin{aligned}
\dot{v}_i^{\text{ON}}(t) &= -v_i^{\text{ON}}(t) + \mu + \xi_i^{\text{ON}}(t), \\
\dot{v}_i^{\text{OFF}}(t) &= -v_i^{\text{OFF}}(t) + \mu + \xi_i^{\text{OFF}}(t) + V_0,
\end{aligned} \tag{2}$$

where $\xi_i^{\text{ON}}(t)$ and $\xi_i^{\text{OFF}}(t)$ are internal noises, and V_0 is the offset of the OFF neurons' activity with respect to the ON neurons [14]. It accounts for the difference in baseline activities of ON and OFF cells. According to Krahe *et al.* [16], this difference is small for baseline rates measured *in vivo*, without external stimulation and with the feedback intact but not causing oscillations. The internal noises are white, zero mean, and Gaussian with intensity D, i.e.,

$$\left\langle \xi_i^k(t) \right\rangle = 0 \quad \text{and} \quad \left\langle \xi_i^k(t)\xi_j^l(t') \right\rangle = 2D\delta_{ij}\delta_{kl}\delta(t - t'),$$

for $i,j = 1,\ldots,N$ and $k,l = \text{ON,OFF}$. Note that the intrinsic noise intensities for ON and OFF cells are identical for the moment, but they will be different in Sec. V B. The brackets $\langle \cdots \rangle$ will always denote ensemble averages.

Sensory pathways to the OFF neurons comprise an interneuron population [11]. It has the approximate effect of

inverting any input coming from the electrosensory afferents. Here, we consider a stochastic input of the form

$$I_i(t) = m + \zeta_i(t)$$

with

$$\zeta_i(t) \equiv \sqrt{c}\eta_c(t) + \sqrt{1-c}\eta_i(t),$$

where η_c is the correlated external noise since it is the same for all neurons, η_i is the uncorrelated external noise, and $m = \langle I_i(t) \rangle$ is the mean stochastic input; all external noises obey the same statistics. For weakly electric fish the stimuli are zero-mean amplitude modulations of their own electric discharge, so we set $m = 0$. It is assumed that these modulations are linearly coded by neural populations innervating the ELL cells [17]. All noise processes are uncorrelated with each other, i.e., $\langle \eta_c \eta_i \rangle = \langle \eta_i \eta_j \rangle = 0$ for all i,j ($i \neq j$) at all times. Note that η_i is the same for each cell in an ON/OFF pair. The correlation parameter $c \in [0,1]$ determines the "weight" of each of the external noise components: The input is fully correlated (fully uncorrelated) if $c = 1$ ($c = 0$). The prefactors $\sqrt{c}$ and $\sqrt{1-c}$ are chosen so that the total input power does not depend on c.

ON and OFF pyramidal cells of the ELL also receive feedback signals from a distant neural population. For simplicity, the signal processing performed by these neurons is a mere average of all the spike trains received from the network, taking into account the axonal propagation time and the filtering due to synaptic transport. The feedback is inhibitory and diffuse, i.e., each cell of the network receives at time t the following feedback input:

$$f(t) = \frac{G}{2N} \int_{\tau_D}^{\infty} \frac{d\tau}{\tau_S} \left(\frac{\tau - \tau_D}{\tau_S} \right) \exp\left(-\frac{\tau - \tau_D}{\tau_S} \right)$$
$$\times \sum_{i=1}^{N} \left[y_i^{ON}(t-\tau) + y_i^{OFF}(t-\tau) \right], \quad (3)$$

where $G < 0$ is the feedback strength [rendering $f(t)$ a negative quantity], τ_S is the decay time, and τ_D is the delay. The spike trains $y_i^{ON}(t)$ and $y_i^{OFF}(t)$ are given by

$$y_i^{\epsilon}(t) = \sum_{t_k} \delta(t - t_k), \quad (4)$$

where the t_k's are the spike times of neuron i ($i = 1, \ldots, N$) of class ϵ ($\epsilon = $ ON, OFF). Thus, the feedback is G times the convolution of a delayed α function [$\Theta(\cdot) = $ Heaviside function]

$$\alpha(\tau) = \frac{1}{\tau_S} \left(\frac{\tau - \tau_D}{\tau_S} \right) \exp\left(-\frac{\tau - \tau_D}{\tau_S} \right) \Theta(\tau - \tau_D)$$

with the population average of the spike trains. The full model is then

$$\dot{v}_i^{ON} = -v_i^{ON} + \mu + \xi_i^{ON} + \zeta_i + f,$$
$$\dot{v}_i^{OFF} = -v_i^{OFF} + \mu + V_0 + \xi_i^{OFF} - \zeta_i + f, \quad (5)$$
$$v(t_k^-) = v_T \Rightarrow t_{spike} = t_k \quad \text{and} \quad v(t_k^+ + \tau_R) = v_R,$$

where we have included the LIF scheme requirements and omitted the dependence of all functions on time for clarity. Note the minus sign in front of ζ_i for the OFF cell equation. A feedforward version ($G = 0$) of this model with ON cells only has been studied in [18,19], with particular emphasis on the

enhancement of pairwise correlations of neurons following an increase of their firing rates.

In this paper, we will mainly be concerned with single-neuron power spectra, cross spectra, and population spectra. The ON and OFF subnetworks are assumed to be separately homogeneous. Therefore, the power spectra are the same for all neurons of the same type and the cross spectra are identical for each neuron pair of the same type. The power spectrum of any neuron is given by

$$S(\omega) = \lim_{T \to \infty} \frac{\langle |\tilde{y}(\omega)|^2 \rangle}{T}, \quad (6)$$

with $\tilde{y}(\omega) = \int_0^T dt\, y(t) e^{i\omega t}$ (we have dropped the ON and OFF superscripts for clarity). The cross spectrum of two neurons is given by

$$S_{cross} = \lim_{T \to \infty} \frac{\langle \tilde{y}_i^*(\omega) \tilde{y}_j(\omega) \rangle}{T}, \quad (7)$$

where both neurons belong to the same class. The average population activity for either the ON or the OFF subnetwork is

$$Y^{ON(OFF)}(t) = \frac{1}{N} \sum_{i=1}^{N} y_i^{ON(OFF)}(t),$$

and the population spectra are just the power spectra of these mean activities. Using the homogeneity of the network, the population spectra of either ON or OFF cells can be expressed in terms of S_{cross} and S [13], namely,

$$S_{pop}(\omega) = S_{cross}(\omega) + \frac{S(\omega) - S_{cross}(\omega)}{N}. \quad (8)$$

III. LINEAR RESPONSE THEORY

Approximate results for the spectral quantities can be obtained using LRT. We write the time evolution of the subthreshold membrane potentials as

$$\dot{v}_i^{ON} = -v_i^{ON} + \mu + \langle f \rangle + \xi_i^{ON} \underline{+ \zeta_i + (f - \langle f \rangle)},$$
$$\dot{v}_i^{OFF} = -v_i^{OFF} + \mu + V_0 + \langle f \rangle + \xi_i^{OFF} \underline{- \zeta_i + (f - \langle f \rangle)}.$$

The underlined terms $\pm\zeta_i + (f - \langle f \rangle)$ are taken as perturbations of the system. The average value of the feedback is $\langle f \rangle = G(r_{ON} + r_{OFF})/2$, with $r_{ON(OFF)} = \langle y_i^{ON(OFF)} \rangle$ being the time-independent mean firing rate of an ON (OFF) neuron [13]. It means that the unperturbed cells have effective biases given by

$$\mu_{ON} = \mu + G(r_{ON} + r_{OFF})/2,$$
$$\mu_{OFF} = \mu + V_0 + G(r_{ON} + r_{OFF})/2. \quad (9)$$

The unperturbed system comprises four relevant parameters, namely, the internal noise intensity D, the effective bias currents μ_{ON} and μ_{OFF}, and the refractory period τ_R. For $\mu_{ON} < v_T$ and $\mu_{OFF} < v_T$, the neurons are in a noise-activated regime [20]. In this case, which will be considered in this paper (except otherwise mentioned), the neurons do not fire at vanishing noise ($r_{ON} = r_{OFF} = 0$) so that the resting potentials are $\bar{v}^{ON} = \mu$ and $\bar{v}_{OFF} = \mu + V_0$. Therefore, increasing (decreasing) V_0 will favor (hinder) the OFF cells' firing once the

noise is set back to a nonzero value. Given the importance of noise in this regime for the neuron firing, it is worth mentioning that the system actually exhibits coherence resonance for some sets of values of the parameters [20]. The cases $\mu_{\mathrm{ON}} > v_T$ and $\mu_{\mathrm{OFF}} > v_T$ are called deterministic firing regimes because the neurons fire in the absence of noise.

A. Unperturbed network

The deviation of the feedback from its mean $(f - \langle f \rangle)$ and the input ζ_i are taken as perturbations of the unperturbed system. When the variances of both these quantities are small, one may assume that the firing rates of the unperturbed system are good approximations to those of the perturbed system [13]. Concretely, this implies that the rates appearing in Eq. (9) may be replaced by the rates obtained from the treatment to follow. A "free" LIF neuron (in open loop and without external input) has a firing rate given by [20]

$$\nu(\mu, D) = \left(\tau_R + \sqrt{\pi} \int_{(\mu-v_T)/\sqrt{2D}}^{(\mu-v_R)/\sqrt{2D}} dx \, e^{x^2} \operatorname{erfc}(x) \right)^{-1}. \quad (10)$$

To get the firing rates of the unperturbed cells, we must replace μ in the above equation by the effective biases of Eq. (9). It results that the rates r_{ON} and r_{OFF} must be determined self-consistently from the coupled equations:

$$\begin{aligned} r_{\mathrm{ON}} &= \nu \left[\mu + G(r_{\mathrm{ON}} + r_{\mathrm{OFF}})/2, D \right], \\ r_{\mathrm{OFF}} &= \nu \left[\mu + V_0 + G(r_{\mathrm{OFF}} + r_{\mathrm{OFF}}] /2, D \right). \end{aligned} \quad (11)$$

Analytical expressions for the unperturbed power spectra ($S_{\mathrm{ON}}^{(0)}$ and $S_{\mathrm{OFF}}^{(0)}$) and the susceptibilities [$A(\omega, \mu_{\mathrm{ON}}, D)$ and $A(\omega, \mu_{\mathrm{OFF}}, D)$] are known [13,21]:

$$S_\epsilon^{(0)} = 2\pi r_\epsilon^2 \delta(\omega) + r_\epsilon \frac{\left| \mathcal{D}_{i\omega}\left(\frac{\mu_\epsilon - v_T}{\sqrt{D}} \right) \right|^2 - e^{2\Delta_\epsilon} \left| \mathcal{D}_{i\omega}\left(\frac{\mu_\epsilon - v_R}{\sqrt{D}} \right) \right|^2}{\left| \mathcal{D}_{i\omega}\left(\frac{\mu_\epsilon - v_T}{\sqrt{D}} \right) - e^{\Delta_\epsilon} e^{i\omega\tau_R} \mathcal{D}_{i\omega}\left(\frac{\mu_\epsilon - v_R}{\sqrt{D}} \right) \right|^2}, \quad (12)$$

$$\begin{aligned} A(\omega, \mu_\epsilon, D) = &\left(\frac{i\omega r_\epsilon}{\sqrt{D}(i\omega - 1)} \right) \\ &\times \left[\frac{\mathcal{D}_{i\omega-1}\left(\frac{\mu_\epsilon - v_T}{\sqrt{D}} \right) - e^{\Delta_\epsilon} \mathcal{D}_{i\omega-1}\left(\frac{\mu_\epsilon - v_R}{\sqrt{D}} \right)}{\mathcal{D}_{i\omega}\left(\frac{\mu_\epsilon - v_T}{\sqrt{D}} \right) - e^{\Delta_\epsilon} e^{i\omega\tau_R} \mathcal{D}_{i\omega}\left(\frac{\mu_\epsilon - v_R}{\sqrt{D}} \right)} \right], \end{aligned} \quad (13)$$

with $\Delta_\epsilon = [v_R^2 - v_T^2 + 2\mu_\epsilon(v_T - v_R)]/4D$ and $\epsilon \in \{\mathrm{ON}, \mathrm{OFF}\}$. The functions $\operatorname{erfc}(x)$ and $\mathcal{D}_a(x)$ are the complementary error function and the parabolic cylinder functions, respectively.

B. Response to the perturbation

A LRT is possible if both the amplitude of the external stimulus and the variance of the feedback are not too large. Then, provided that the internal noise is large, the following ansatz can be made for the perturbed spike trains [12,13,22–24]:

$$y_i^\epsilon(t) = y_{\epsilon,i}^{(0)}(t) + [A(\mu_\epsilon, D) \star (\epsilon\zeta_i + f - \langle f \rangle)](t). \quad (14)$$

Here and in the following, ϵ as a subscript or superscript will stand for ON or OFF; as a multiplicative constant, it stands for $+$ in an expression for an ON variable or $-$ for an OFF

variable. The $\star$ denotes the convolution operation and the $y_{\epsilon,i}^{(0)}$'s are the unperturbed spike trains. Taking the Fourier transform on each side, we get for $\omega \neq 0$ [25],

$$\begin{aligned} \tilde{y}_i^\epsilon(\omega) = &\, \tilde{y}_{\epsilon,i}^{(0)}(\omega) + A(\omega, \mu_\epsilon, D) \\ &\times \left[\epsilon\tilde{\zeta}_i(\omega) + \frac{F(\omega)}{2N} \left(\sum_{k=1}^N \tilde{y}_k^{\mathrm{ON}}(\omega) + \sum_{k=1}^N \tilde{y}_k^{\mathrm{OFF}}(\omega) \right) \right] \end{aligned} \quad (15)$$

with

$$F(\omega) = G\alpha(\omega) = G \frac{e^{i\omega\tau_D}}{(1 - i\omega\tau_S)^2} \quad (16)$$

as the Fourier transform of the delayed α function times the feedback strength G.

C. Calculation of spectral quantities

To compute the relevant spectral quantities, we first form the subsidiary sums:

$$\tilde{Y}_\epsilon^{(0)} = \frac{1}{N} \sum_{i=1}^N \tilde{y}_{\epsilon,i}^{(0)}, \quad \tilde{Y}_\epsilon = \frac{1}{N} \sum_{i=1}^N \tilde{y}_i^\epsilon, \quad \tilde{\zeta} = \frac{1}{N} \sum_{i=1}^N \tilde{\zeta}_i. \quad (17)$$

Summing Eq. (15) over i from 1 to N and dividing by N, we get, writing $A(\omega, \mu_\epsilon, D) \equiv A_\epsilon$,

$$\tilde{Y}_\epsilon = \tilde{Y}_\epsilon^{(0)} + \epsilon A_\epsilon \tilde{\zeta} + \frac{A_\epsilon F}{2}(\tilde{Y}_{\mathrm{ON}} + \tilde{Y}_{\mathrm{OFF}}).$$

These two equations (one for each value of ϵ) can be used to get an expression for the sum $\tilde{Y}_{\mathrm{ON}} + \tilde{Y}_{\mathrm{OFF}}$ intervening in Eq. (15). We now have workable expressions for the Fourier transform of the spike trains:

$$\tilde{y}_i^\epsilon = \tilde{y}_{\epsilon,i}^{(0)} + A_\epsilon \left[\epsilon\tilde{\zeta}_i + \gamma \left(\tilde{Y}_{\mathrm{ON}}^{(0)} + \tilde{Y}_{\mathrm{OFF}}^{(0)} \right) + \gamma (A_{\mathrm{ON}} - A_{\mathrm{OFF}})\tilde{\zeta} \right] \quad (18)$$

with

$$\gamma = \frac{F/2}{1 - \frac{(A_{\mathrm{ON}} + A_{\mathrm{OFF}})}{2} F}. \quad (19)$$

From Eq. (18), it is seen that the perturbed spike train is made of the response of the single neuron to both its external input and to the network's overall activity processed by the feedback kernel.

The following properties are essential to the computation of the spectral quantities:

(1) Unperturbed spike trains are uncorrelated with the external stimuli:

$$\lim_{T \to \infty} \frac{\langle \tilde{y}_{\epsilon,i}^{(0)*} \tilde{\eta}_j \rangle}{T} = \lim_{T \to \infty} \frac{\langle \tilde{y}_{\epsilon,i}^{(0)*} \tilde{\eta}_c \rangle}{T} = 0, \quad \forall i, j.$$

(2) Unperturbed spike trains are uncorrelated among each other ($\omega \neq 0$):

$$\lim_{T \to \infty} \frac{\langle \tilde{y}_{\epsilon,i}^{(0)*} \tilde{y}_{\epsilon,j}^{(0)} \rangle}{T} = S_\epsilon^{(0)} \delta_{ij}, \quad \lim_{T \to \infty} \frac{\langle \tilde{y}_{\epsilon,i}^{(0)*} \tilde{y}_{-\epsilon,j}^{(0)} \rangle}{T} = 0, \quad \forall i, j,$$

where we have written $-\epsilon$ to signify that if $\epsilon = \mathrm{ON}$, $-\epsilon = \mathrm{OFF}$ and conversely.

(3) The external stimuli satisfy

$$\lim_{T\to\infty}\frac{\langle\tilde{\eta}_i^*\tilde{\eta}_j\rangle}{T}=S_{\text{st}}\delta_{ij}, \quad \lim_{T\to\infty}\frac{\langle|\tilde{\eta}_c|^2\rangle}{T}=S_{\text{st}},$$

$$\lim_{T\to\infty}\frac{\langle\tilde{\eta}_i^*\tilde{\eta}_c\rangle}{T}=0, \quad \forall i,j,$$

with S_{st} the statistics of the noise inputs, which will be described in Sec. IV.

After algebraic manipulations, the single-neuron power spectra read ($\text{Re}(\cdot)=$ real part of $\cdot$)

$$S_\epsilon = S_\epsilon^{(0)}\left[1+\frac{2}{N}\text{Re}\,(\gamma A_\epsilon)+\frac{|\gamma A_\epsilon|^2}{N}\right]+S_{-\epsilon}^{(0)}\frac{|\gamma A_\epsilon|^2}{N}$$

$$+|A_\epsilon|^2 S_{\text{st}}\left\{1+\left[\frac{1}{N}(1-c)+c\right]\right.$$

$$\left.\times[2\,\text{Re}[\gamma(A_\epsilon-A_{-\epsilon})]+|\gamma(A_\epsilon-A_{-\epsilon})|^2]\right\}, \quad (20)$$

where we have used the facts that $\epsilon(A_{\text{ON}}-A_{\text{OFF}})=A_\epsilon-A_{-\epsilon}$ and $|A_{\text{ON}}-A_{\text{OFF}}|^2=|A_\epsilon-A_{-\epsilon}|^2$. Again $\omega\neq0$, and $S_\epsilon^{(0)}$ stands for the second term only of Eq. (12). In the large N limit, the only terms remaining are the power spectrum of the response of a single neuron to the total external noise $(S_\epsilon^{(0)}+|A_\epsilon|^2 S_{\text{st}})$ and the term

$$c|A_\epsilon|^2 S_{\text{st}}[2\,\text{Re}\,[\gamma(A_\epsilon-A_{-\epsilon})]+|\gamma(A_\epsilon-A_{-\epsilon})|^2], \quad (21)$$

which represents the effect of the network response to the correlated noise. The contribution from the identically distributed uncorrelated noises filtered by the feedback kernel vanishes in this limit. Still in this limit, $c=0$ causes the feedback to have the sole effect of shifting the bias current, i.e., only the static part of the feedback matters.

If the offset $V_0=0$, $\mu_{\text{ON}}=\mu_{\text{OFF}}$. Hence $A_{\text{ON}}=A_{\text{OFF}}$ and $S_{\text{ON}}^{(0)}=S_{\text{OFF}}^{(0)}$, and the correlation parameter c has no effect on the spectrum, even at finite N. We thus see that within the limits of applicability of the LRT, introducing the OFF cells into the system cancels the effect of the spatial correlation of the external input.

The cross spectrum of two ON or two OFF neurons, noted $S_{\text{cross}}^\epsilon$, is

$$S_{\text{cross}}^\epsilon = S_\epsilon^{(0)}\left[\frac{2}{N}\text{Re}\,(\gamma A_\epsilon)+\frac{|\gamma A_\epsilon|^2}{N}\right]+S_{-\epsilon}^{(0)}\frac{|\gamma A_\epsilon|^2}{N}$$

$$+|A_\epsilon|^2 S_{\text{st}}\left\{c+\left[\frac{1}{N}(1-c)+c\right]\right.$$

$$\left.\times[2\,\text{Re}[\gamma(A_\epsilon-A_{-\epsilon})]+|\gamma(A_\epsilon-A_{-\epsilon})|^2]\right\}$$

$$= S_\epsilon - S_\epsilon^{(0)}-(1-c)|A_\epsilon|^2 S_{\text{st}}. \quad (22)$$

The cross spectrum is thus given by the difference between the perturbed power spectrum, on the one hand, and the unperturbed spectrum of the neuron plus the transmitted uncorrelated noise, on the other hand. It means that the feedback term has the same effect on both the single-neuron power spectrum and the cross spectrum, just like for the ON-only network [13]. For a fully correlated input ($c=1$), $S_{\text{cross}}^\epsilon$ is a measure of the difference between the perturbed and the unperturbed single-neuron spectra.

IV. THEORY FOR GAUSSIAN WHITE NOISE STIMULI OF UNLIMITED BANDWIDTH

Until now, the statistics of the external noises have been left unspecified. For the LRT to be valid, both the variance of these noises and the feedback strength must be small compared to the internal noise. Following [13], we will paradoxically consider Gaussian white noise stimuli of unlimited bandwidth for both the uncorrelated and the correlated noises:

$$\langle\eta_c(t)\eta_c(t')\rangle=\langle\eta_i(t)\eta_i(t')\rangle=2D_E\delta(t-t'). \quad (23)$$

The variance is infinite for white noise and thus does not meet the above requirements. Lindner and co-workers [13] circumvent this difficulty by making the following ansatz: Whenever $S_\epsilon^{(0)}(\omega,D)+2D_E|A_\epsilon(\omega,D)|^2$ appears in the expressions for the spectral measures, one may replace it approximately by

$$S_\epsilon^{(0)}(\omega,Q)\equiv S_{\epsilon,Q}^{(0)}, \quad (24)$$

with $Q=D+D_E$ the total noise intensity perceived by the neurons. It is also understood that the susceptibilities $A_\epsilon(\omega,D)$ must be replaced by $A_\epsilon(\omega,Q)\equiv A_{\epsilon,Q}$, and $\gamma(\omega,D)$ becomes

$$\gamma_Q=\frac{F/2}{1-\frac{A_{\text{ON},Q}+A_{\text{OFF},Q}}{2}F}. \quad (25)$$

The firing rates also need to be evaluated at noise intensity Q: $r_\epsilon^{(0)}(\mu_\epsilon,D)\to r_\epsilon^{(0)}(\mu_\epsilon,Q)$. The informal argument behind these substitutions is that a neuron should not make the difference between the statistics of external and internal noises if they are the same. See Lindner *et al.* [13] for more details. Doing so, we get for the single neuron power spectra,

$$S_{\epsilon,Q}(\omega)$$

$$= S_{\epsilon,Q}^{(0)}\left(1+\frac{2}{N}\text{Re}(\gamma_Q A_{\epsilon,Q})+\frac{1}{N}|\gamma_Q A_{\epsilon,Q}|^2\right)$$

$$+S_{-\epsilon,Q}^{(0)}\frac{1}{N}|\gamma_Q A_{\epsilon,Q}|^2+2D_E|A_{\epsilon,Q}|^2\left(\frac{1}{N}(1-c)+c\right)$$

$$\times\{2\,\text{Re}[\gamma_Q(A_{\epsilon,Q}-A_{-\epsilon,Q})]+|\gamma_Q(A_{\epsilon,Q}-A_{-\epsilon,Q})|^2\}$$

$$-2D_E|A_{\epsilon,Q}|^2\left[\frac{2}{N}\text{Re}(\gamma_Q A_{\epsilon,Q})\right.$$

$$\left.+\frac{1}{N}|\gamma_Q A_{\epsilon,Q}|^2+\frac{1}{N}|\gamma_Q A_{-\epsilon,Q}|^2\right]. \quad (26)$$

Cross spectra of neurons within a given subpopulation are readily computed by making the appropriate substitutions in Eq. (22):

$$S_{\text{cross},Q}^\epsilon = S_{\epsilon,Q}-S_{\epsilon,Q}^{(0)}+2cD_E|A_{\epsilon,Q}|^2, \quad (27)$$

and likewise for the population spectra S_{pop}^ϵ.

Numerical integrations of Eq. (5) for a particular set of parameters were done using a simple Euler scheme with $\Delta t=5\times10^{-4}$ and between 100 and 200 realizations. The Gaussian white noise used in the simulations is intrinsically bandlimited to the Nyquist frequency, which is 2×10^5 Hz for a membrane time constant of 5 ms.

V. RESULTS

A. Symmetric case

Above, we noted that for $V_0 = 0$, the ON and OFF susceptibilities and unperturbed spectra are equal. In this symmetric case, Eq. (20) becomes (replacing γ by its expression and rearranging)

$$S_\epsilon = S_\epsilon^{(0)} + |A_\epsilon|^2 S_{st} + \frac{S_\epsilon^{(0)}}{2N} \frac{2\,\mathrm{Re}(A_\epsilon F) - |A_\epsilon F|^2}{|1 - A_\epsilon F|^2}. \quad (28)$$

We compare the above equation with $\epsilon = \mathrm{ON}$ to the LRT power spectrum for the ON-only network [[13], Eq. (22)] that we reproduce here for convenience:

$$S = S_0 + |A|^2 S_{st} + c|A|^2 S_{st} \frac{2\,\mathrm{Re}(AF) - |AF|^2}{|1 - AF|^2}$$
$$+ \frac{1}{N}[S_0 + (1-c)|A|^2 S_{st}] \frac{2\,\mathrm{Re}(AF) - |AF|^2}{|1 - AF|^2}.$$

Here, N is the total number of neurons, whereas N in Eq. (28) is the number of cells of a given type. For $c = 0$ and large N, both expressions are similar if our N is chosen to be equal to half the number of cells in the ON-only network. Figure 2(a)

illustrates this fact: The LRT curves are superposed except for a small interval near $\omega = 1.5$, where the LRT for the ON-only network is very slightly higher (see inset). On this same plot the corresponding small bump in the numerical curve for the ON/OFF network is difficult to see.

For the case $c = 1$, a drastic contrast is seen between the network types, as depicted in Fig. 2(b). As in [13], the ON-only network undergoes strong gamma oscillations, embodied in the strong peak at $\omega = 1.5$. However, they are nearly absent for the ON/OFF network. Note that for a membrane time constant of 5 ms, the frequency of the peak corresponds to 48 Hz (for comparison, [9] uses 6 ms and [7], 10 ms). The agreement between the LRT and the numerical results is excellent, although there are minor quantitative discrepancies at low frequency (especially in the case $c = 1$).

At this point, it is also worth noting that adding more neurons yields weaker oscillations in both the ON-only [13] and the ON/OFF network (not shown), although they survive for the ON-only network for $N \to \infty$. So, had we chosen a different number of neurons of each type (e.g., setting $N_{\mathrm{ON}} = N_{\mathrm{OFF}} = 100$), the conclusion regarding the weakening of oscillations would have been qualitatively the same.

Perhaps a better way to ascertain the occurrence (or not) of network oscillations is to consider population spectra, as is done in Fig. 3(a). For a correlated input, one can see a high peak at $\omega = 1.5$ for the ON-only spectrum and a significantly lower peak at about the same frequency for the ON/OFF network. The correlated input triggers high correlations between the spike trains for the ON-only network; for the ON/OFF
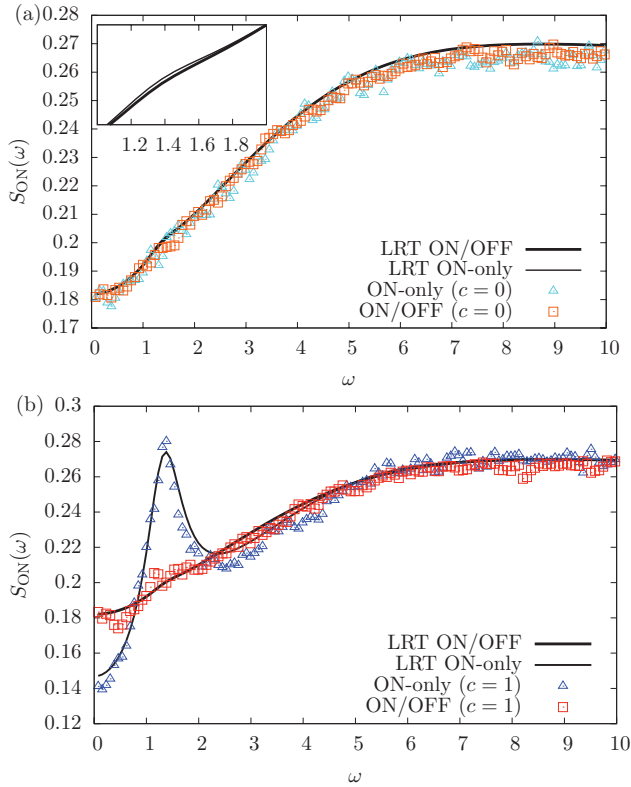

FIG. 2. (Color online) Impact of OFF cells on gamma oscillations. Power spectra of ON cells for both the ON-only network ($N = 100$) and the ON/OFF network ($N_{\mathrm{ON}} = N_{\mathrm{OFF}} = 50$) are displayed for uncorrelated [$c = 0$, plot (a)] and correlated [$c = 1$, plot (b)] inputs. The inset in plot (a) shows the difference between the LRT curves for the ON-only and the ON/OFF networks for $1 < \omega < 2$. Parameters are $\mu = 0.8$, $D = 0.12$, $D_E = 0.08$, $V_0 = 0$, $\tau_D = 1$, $\tau_S = 0.5$, $\tau_R = 0.1$, and $G = -1.2$; these are the same values as in Fig. 2 of [13] (note the labeling error on that figure). The triangles and squares are from numerical simulations; LRT, linear response theory.
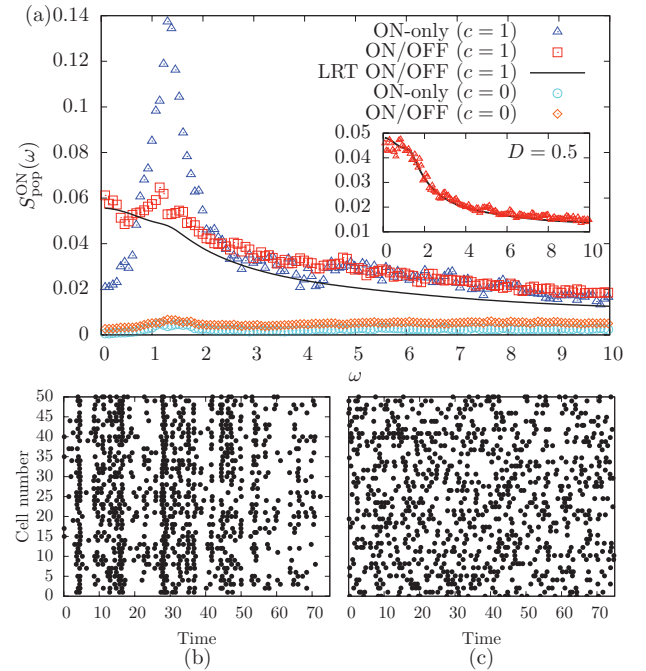

FIG. 3. (Color online) Impact of OFF cells on population activity. (a) Comparison of ON population spectra for the ON-only and ON/OFF networks. Parameters are the same as in Fig. 2. The only LRT curve displayed is for the ON/OFF network with $c = 1$ (see text for explanation). Inset: LRT for higher internal noise. (b) and (c) Raster plots for ON neurons in the ON/OFF network with $c = 1$ (b) and $c = 0$ (c).
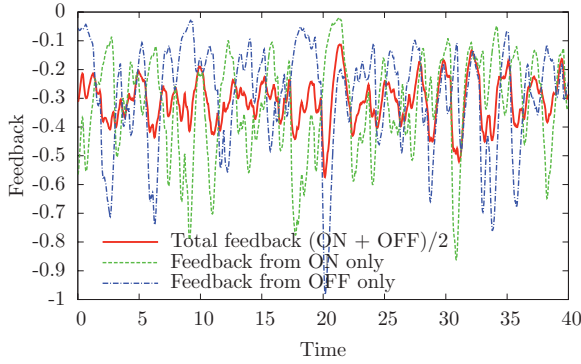
FIG. 4. (Color online) Time course of the feedback due to ON (green dashed curve) and OFF (blue dot-dashed curve) cells and of the total feedback (solid red curve) during one realization. Observe that the peaks and troughs of the blue (dot-dashed) and green (dashed) traces are roughly in antiphase.

network, the correlations between ON cells are impeded by the OFF cells, which respond in an opposite way to the external Gaussian noise. In the case $c = 0$ the power is small at each frequency (lowest curves). The slight bump around $\omega = 1.5$ does not represent significant collective oscillations since the power is everywhere small. The vanishing of network oscillations is confirmed by looking at the raster plots in Figs. 3(b) and 3(c): No stripes of quasisynchronous spikes are seen in the case $c = 0$.

For a large number of neurons, in both the ON/OFF and ON-only cases, the population spectrum is approximately equal to the cross spectrum [see Eq. (8)]. Since the cross spectrum is inherently a two-neuron quantity, and given that its evaluation through the LRT implies the use of single-neuron quantities only, the LRT usually fails to reproduce the population spectra (see again [13] for a thorough discussion). An example is provided in Fig. 3(a) (compare the red squares with the black curve). A better fit is obtained for higher internal noise intensities, as exemplified in the inset. This is due to a decrease of the correlations and to the linearization effect of a high internal noise, so that a LRT will represent more adequately the behavior of the system.

The reason behind the vanishing of network oscillations in the symmetric case is that the ON and OFF cells are totally opposite in their spectral response: When, say, an ON cell has just received the sufficient input to cross the threshold, the probability that the OFF cell in the same pair should fire should be low. This is perhaps best envisioned in Fig. 4, where we have plotted the feedback from the ON and the OFF cells for a single trial, together with the total feedback from the kernel. The feedback due to the ON (OFF) cells is a low-pass filtered version of the time-varying ON (OFF) firing rate. The oscillations of these feedbacks are roughly in antiphase and produce a reduced modulation of the network's activity. To put it into the language of [7], the waves of inhibition coming from the feedback kernel are reduced in amplitude due to the antagonistic response of the two classes of cells to external inputs. We further add that, from the dynamical systems perspective, it has been shown that the inclusion of OFF-type responses in continuous neural networks shifts the threshold for oscillatory instabilities under deterministic

stimulation [14]. We conclude that we observe here the same phenomenon in a fully noisy and spiking framework.

In the following sections, we try to get back the strong gamma oscillations seen for the ON-only network under global stimulation by introducing asymmetries between the ON and the OFF cells. First, we will set the offset $V_0 > 0$ with a reduced intrinsic noise for the OFF cells. Then, we will consider unequal membrane time constants, again with $V_0 > 0$. The latter case requires a more delicate analytical treatment. Note that the parameters $G = -1.2, \tau_D = 1, \tau_S = 0.5$, and $\tau_R = 0.1$ will stay fixed to these values for the remainder of this paper to allow comparison with results from the symmetric case and the ON-only network. However, we would expect our conclusions to be more generally valid. From [13], we know that gamma oscillations are present over a certain part of parameter space for the ON-only network. Suppose that there is a gamma peak in the ON-only case for a given set of parameters (with $c = 1$). Then, provided that these parameter values are such that the LRT remains a valid approximation, Eq. (20) stipulates that gamma-band oscillations should be greatly reduced for the corresponding ON/OFF network in the symmetric case. Moreover, the symmetry breakings discussed below have precise effects on ON and OFF cells. Although we did not explore the full extent of parameter space in search of counterexamples, we suspect these effects—on the grounds of the LRT—to be generic rather than mere artifacts of the given choice of parameter values.

B. Asymmetry between ON and OFF cells: Offset and OFF cells' intrinsic noise

As stated in Sec. II, physiological experiments have shown that the spontaneous—without external stimulation and with intact feedback—firing rates of ON and OFF cells are approximately the same on average [16]. Also, on average, ON cells have higher spike thresholds (V_T) than OFF cells [26]. For comparable resting and reset potentials for both classes of cells, it would mean, because of Eq. (1), that the ON bias current is smaller than that of OFF cells. To account for the larger bias of OFF cells, we try in the present section to increase the offset V_0 of OFF cells. As shown in Appendix A, the ON (OFF) rate is a monotonically decreasing (increasing) function of V_0. For the rates of ON and OFF cells to stay equal, another parameter must be changed concomitantly with V_0. One possibility is to reduce the internal noise intensity of OFF cells, which will be denoted by D_{OFF}. This implies that the OFF cells are now more deterministic than the ON cells and will fire more reliably.

Figures 5(a) and 5(b) show power spectra for different values of the offset when $c = 1$. In Fig. 5(a), we also display the corresponding power spectrum for the ON-only network, showing an obvious gamma peak. The ON cells' power spectra are nearly identical for all values of V_0. The inset of Fig. 5(a) shows that there exists a minute difference between the LRT curves around the vanished gamma peak. On the contrary, for OFF cells, a salient contrast appears between the spectra when the offset increases. Going from $V_0 = 0$ to $V_0 = 0.3$, the OFF cells progressively transfer power from low to high frequency. This is in line with what should happen to a LIF neuron becoming more deterministic. From renewal theory,
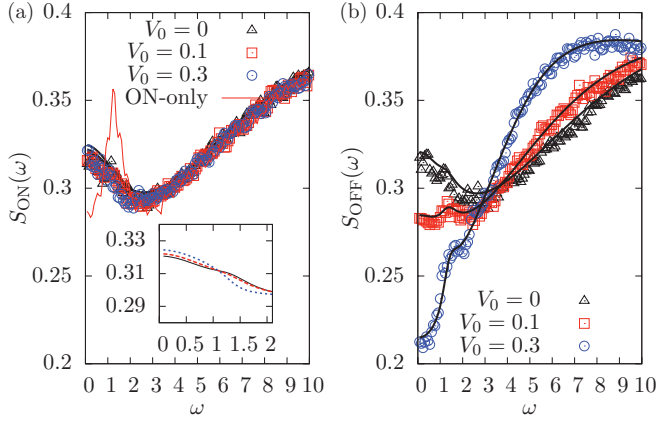
FIG. 5. (Color online) ON (a) and OFF (b) power spectra for different values of V_0, with the ON internal noise intensity $D_{\mathrm{ON}} = 0.36$ and $c = 1$. The OFF cells' internal noise intensity D_{OFF} is decreased so that the rates remain the same within an absolute error of order 10^{-3}. The values of D_{OFF} for $V_0 = 0, 0.1, 0.3$ are, respectively, $D_{\mathrm{OFF}} = 0.36, 0.27, 0.125$. All other parameters are as in Fig. 2. On plot (a), we also show the power spectrum for the corresponding ON-only network (solid red curve with a distinguishable peak). The inset shows the difference between the LRT curves around $\omega = 1.5$ (solid black, $V_0 = 0$; dashed red, $V_0 = 0.1$; and dotted blue, $V_0 = 0.3$). Other LRT curves are black and fit the numerical results. Note that the effective bias currents stay well below v_T for all curves.

we know that the coefficient of variation (C_V) is given by [20]

$$C_V = \sqrt{\frac{\lim_{\omega \to 0} S_{\mathrm{OFF}}(\omega)}{\lim_{\omega \to \infty} S_{\mathrm{OFF}}(\omega)}}. \tag{29}$$

From inspection of Fig. 5(b), we see that the C_V decreases for increasing offsets, meaning that greater regularity is achieved by the OFF cells. But this analysis is applicable only if the perturbed spike train does not depart too much from a renewal process. The unperturbed spike train is clearly a renewal process [20], but the perturbed one should not be, because of the feedback. From Eq. (22) with $c = 1$, $S_{\mathrm{cross}}^{\mathrm{OFF}} = S_{\mathrm{OFF}} - S_{\mathrm{OFF}}^{(0)}$ and, from Eq. (8), $S_{\mathrm{pop}}^{\mathrm{OFF}} \approx S_{\mathrm{cross}}^{\mathrm{OFF}}$. Hence, in the large N limit we have

$$S_{\mathrm{OFF}} \approx S_{\mathrm{OFF}}^{(0)} + S_{\mathrm{pop}}^{\mathrm{OFF}}. \tag{30}$$

Therefore, the extent to which the perturbed spike train departs from a renewal process—with the proviso that Eq. (22) comes from the LRT—is dictated by the values of $S_{\mathrm{pop}}^{\mathrm{OFF}}$ [see Fig. 6(b)]. The maximum value of the ratio $S_{\mathrm{pop}}^{\mathrm{OFF}}/S_{\mathrm{OFF}}$ is about 0.35 for $V_0 = 0.3$. We are thus tempted to analyze the results of Fig. 5(b) in the following way: Upon an increase of the offset, the OFF cells become intrinsically more regular due to the larger effective bias, and this allows for the feedback-induced oscillations to gain in power, in comparison to the power of the unperturbed spike train.

The recovery of gamma oscillations for the OFF cells is really a network effect induced by the common action of the feedback and the correlated input. This is clear from Figs. 6(b) and 6(d). The correlations between gamma-frequency Fourier components increase with V_0, with a maximum around $\omega = 1.5$ [Fig. 6(b)]. The cells also tend to synchronize, as
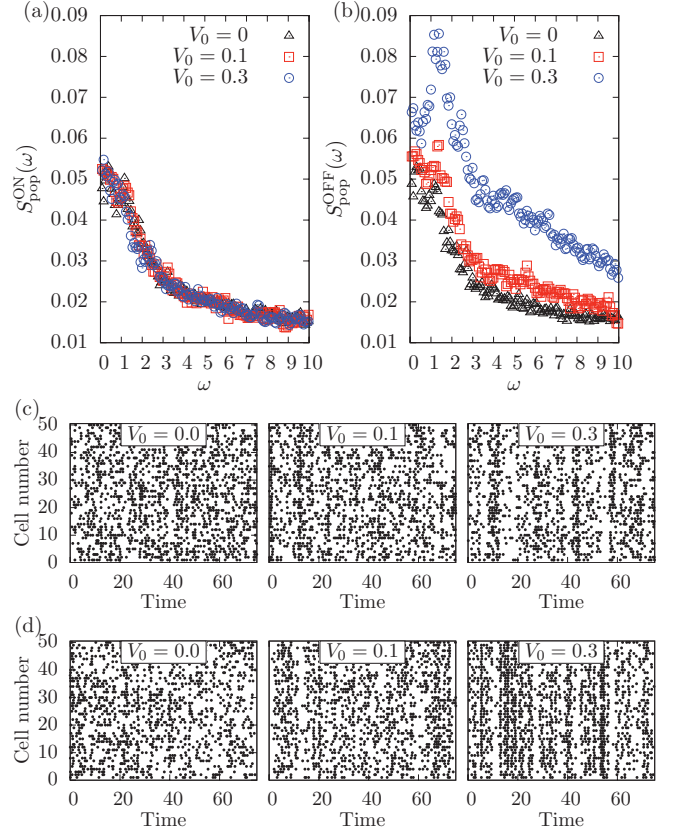

FIG. 6. (Color online) Population spectra for ON (a) and OFF cells (b) corresponding to Fig. 5 for the ON/OFF network. (c) and (d) are raster plots for ON and OFF cells, respectively. The spectral correlations ($S_{\mathrm{cross}}^{\mathrm{OFF}} \approx S_{\mathrm{pop}}^{\mathrm{OFF}}$) are enhanced for increasing offsets for the OFF cells (b), but not for the ON cells (a). The raster plots of panel (d) show the enhanced synchronization of OFF cells with increasing V_0.

revealed by the appearance of well-defined stripes in Fig. 6(d) for $V_0 = 0.3$.

The ON cells' behavior is more enigmatic. Both the single-neuron and the population spectra do not seem to change, as per the numerical results of Figs. 5(a) and 6(a). In the inset to Fig. 5(a), however, the LRT curves show a small decrease of power with increasing V_0 around the gamma frequency, to the advantage of the lower frequencies. Also, in Fig. 6(c), one may notice a hint of attempted synchronization for $V_0 = 0.3$. Comparing Figs. 6(c) and 6(d) for $V_0 = 0.3$, we see that whenever the OFF cells are firing, the ON cells are not. When the OFF cells have just received the sufficient push to cross the firing threshold, ON cells receive an opposite external drive which will cause their firing to be less likely. Given that the OFF cells strongly oscillate collectively, the ON cells are bound to their activity. However, the latter do not show gamma oscillations per se because they lack a gamma peak in the power spectrum. This is different than the experimental situation where both the ON and OFF cells show gamma oscillations [7]. The slight increase in oscillatory strength for the ON/OFF network is compatible with the neural field prediction that an increase in V_0 can enhance the propensity of the deterministic ON/OFF system to exhibit oscillations [[15], Fig. 4(c)], although in that case the rates are not constrained to be equal.

C. Asymmetry between ON and OFF cells: Unequal membrane time constants

Studies of mutual information and coherence between spike trains and Gaussian noise have shown that OFF cells are low pass under local stimulus for all maps constituting the ELL [16,26,27]. This means that OFF cells tend to respond more to the low-frequency components of the stimulus. The ON cells are more heterogenous across the maps and can be low pass, broadband, and even high pass [26]. Thus, on average, the OFF cells are more low pass than the ON cells. One way to account for this is to reconsider the assumption that we have made hitherto, i.e., that the membrane time constants of ON and OFF neurons are equal. Slower membrane dynamics are likely to promote the low-frequency components of the input. Mathematically, this implies that we consider the following dynamics for the unperturbed OFF membrane potentials:

$$\tau_{\text{ratio}}\dot{v}_i^{\text{OFF}}(t) = -v_i^{\text{OFF}}(t) + \mu_{\text{OFF}} + \xi_i^{\text{OFF}}(t), \quad (31)$$

with $\tau_{\text{ratio}} \equiv \tau_{\text{OFF}}/\tau_{\text{ON}}$ the ratio of the membrane time constants. The internal noises are equal as before. Analytical formulas for the rates and spectra of the unperturbed system are given for LIF equations of the form $\dot{v} = -v + \mu + \xi(t)$. The above equation is evidently not of this form. To get rid of the τ_{ratio} prefactor, we define $\hat{t} = t/\tau_{\text{ratio}}$. The consequence is to rescale (1) the noise intensity, $D \rightarrow \hat{D} = D/\tau_{\text{ratio}}$; (2) the various time constants of the model,

$$\hat{\tau}_R = \frac{\tau_R}{\tau_{\text{ratio}}}, \quad \hat{\tau}_D = \frac{\tau_D}{\tau_{\text{ratio}}}, \quad \hat{\tau}_S = \frac{\tau_S}{\tau_{\text{ratio}}};$$

and (3) the feedback strength, $\hat{G} = G/\tau_{\text{ratio}}$.

Evidently, the use of these new constants demands corresponding modifications of the spectral quantities. The steps leading to the LRT in the presence of unequal membrane time constants are given in Appendix B. We get for the unperturbed power spectrum [see Eq. (B7)]

$$S_{\text{OFF}}^{(0)}$$
$$= r_{\text{OFF}} \frac{\left|\mathcal{D}_{i\tau_{\text{ratio}}\omega}\left(\frac{\mu_{\text{OFF}}-v_T}{\sqrt{D/\tau_{\text{ratio}}}}\right)\right|^2 - e^{2\tau_{\text{ratio}}\Delta_{\text{OFF}}}\left|\mathcal{D}_{i\tau_{\text{ratio}}\omega}\left(\frac{\mu_{\text{OFF}}-v_R}{\sqrt{D/\tau_{\text{ratio}}}}\right)\right|^2}{\left|\mathcal{D}_{i\tau_{\text{ratio}}\omega}\left(\frac{\mu_{\text{OFF}}-v_T}{\sqrt{D/\tau_{\text{ratio}}}}\right) - e^{\tau_{\text{ratio}}\Delta_{\text{OFF}}}e^{i\omega\tau_R}\mathcal{D}_{i\tau_{\text{ratio}}\omega}\left(\frac{\mu_{\text{OFF}}-v_R}{\sqrt{D/\tau_{\text{ratio}}}}\right)\right|^2}$$

and for the susceptibility [cf. Eq. (B8)]

$$A_{\text{OFF}}$$
$$= \left(\frac{i\tau_{\text{ratio}}\omega r_{\text{OFF}}}{\sqrt{D/\tau_{\text{ratio}}}(i\tau_{\text{ratio}}\omega - 1)}\right)$$
$$\times \left[\frac{\mathcal{D}_{i\tau_{\text{ratio}}\omega-1}\left(\frac{\mu_{\text{OFF}}-v_T}{\sqrt{D/\tau_{\text{ratio}}}}\right) - e^{\tau_{\text{ratio}}\Delta_{\text{OFF}}}\mathcal{D}_{i\tau_{\text{ratio}}\omega-1}\left(\frac{\mu_{\text{OFF}}-v_R}{\sqrt{D/\tau_{\text{ratio}}}}\right)}{\mathcal{D}_{i\tau_{\text{ratio}}\omega}\left(\frac{\mu_{\text{OFF}}-v_T}{\sqrt{D/\tau_{\text{ratio}}}}\right) - e^{\tau_{\text{ratio}}\Delta_{\text{OFF}}}e^{i\omega\tau_R}\mathcal{D}_{i\tau_{\text{ratio}}\omega}\left(\frac{\mu_{\text{OFF}}-v_R}{\sqrt{D/\tau_{\text{ratio}}}}\right)}\right].$$
$$(32)$$

In Sec. B 2 of Appendix B, we prove that r_{OFF} decreases when τ_{ratio} is increased at fixed V_0. Therefore, to fulfill the constraint of equal ON and OFF rates, V_0 must be increased concurrently with τ_{ratio}. For $\tau_{\text{ratio}} = 1$ and $V_0 = 0$, $r_{\text{ON}} = r_{\text{OFF}}$. Now, we have to suppose that as we increase τ_{ratio}, we also increase V_0 so that the rates stay the same (numerically, they will remain the same within statistical error). This means that $\mu_{\text{OFF}} = \mu + V_0 + Gr_{\text{ON}}$ increases with τ_{ratio}, whereas μ_{ON} remains the same. Also, $\hat{D}$ diminishes with increasing

τ_{ratio}. Hence, the unperturbed activity of the OFF cells tends more and more towards the deterministic firing regime as τ_{ratio} is increased from 1, with the possibility of bifurcating to the deterministic regime at $\mu_{\text{OFF}} = 1$. Finally, given the presence of $\tau_{\text{ratio}}\omega$ instead of ω as a subscript of the parabolic cylinder functions, the unperturbed spectrum will also have the tendency to be compressed toward the $\omega = 0$ axis for large τ_{ratio}. But this compression is not trivial due to the presence of the exponential term $\exp(i\omega\tau_R)$ in the expression above. Something similar is expected for the susceptibility.

We now want to study the effect of τ_{ratio} on the coherence of OFF cells. In the Introduction, we stated that local and spatially uncorrelated global stimuli seem to have similar impacts on ELL neurons. Hence, we here use a global stimulus with $c = 0$. Exceptionally, the external Gaussian noise is bandlimited to 0–120 Hz. The coherence is given by [28]

$$C(\omega) = \frac{\left|S_{\eta_i y_i}(\omega)\right|^2}{S_{\text{OFF}}(\omega)S_{\text{st}}(\omega)}, \quad (33)$$

where $S_{\eta_i y_i}(\omega)$ is the cross spectrum between the spatially uncorrelated noise and the spike train given by Eq. (20). Using the LRT to express the various quantities in Eq. (33), we get in the limit $N \rightarrow \infty$,

$$C(\omega) = \frac{|A_{\text{OFF}}(\omega)|^2 S_{\text{st}}(\omega)}{S_{\text{OFF}}^{(0)}(\omega) + |A_{\text{OFF}}(\omega)|^2 S_{\text{st}}(\omega)}. \quad (34)$$

Figure 7 shows the effect of τ_{ratio} on the coherence as a function of ω for two special cases: In Fig. 7(a), the bias μ is high and D is low, and conversely for Fig. 7(b). In both cases, it is obvious that the OFF cells become more low pass as τ_{ratio} is increased. For $\tau_{\text{ratio}} = 1$, $A_{\text{ON}} = A_{\text{OFF}}$ and $S_{\text{ON}}^{(0)} = S_{\text{OFF}}^{(0)}$, therefore the red curves of Fig. 7 also represent the coherence of the ON cells.
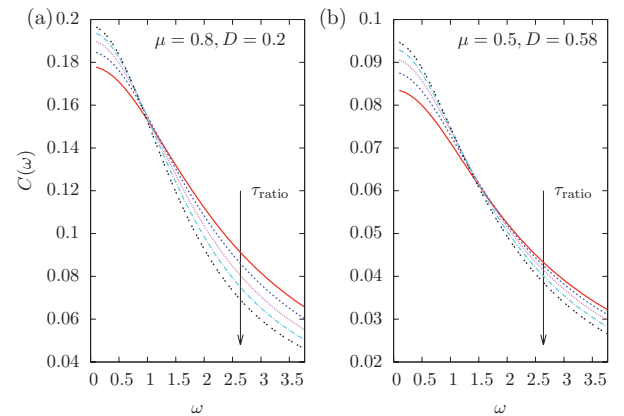

FIG. 7. (Color online) Coherence of OFF cells—computed using Eq. (34)—for different τ_{ratio} with spatially uncorrelated input ($c = 0$) and in the limit $N \rightarrow \infty$. V_0 has been adjusted so that $r_{\text{ON}} = r_{\text{OFF}}$ within an absolute error of order 10^{-3}. Arrow indicates the direction of increasing τ_{ratio}; τ_{ratio} starts at 1 (solid red curves) and stops at 1.8 (double-dotted black curves) with increments of 0.2. Values for μ and D are (a) $\mu = 0.8$, $D = 0.2$ and (b) $\mu = 0.5$, $D = 0.58$. For (a), the effective biases range from 0.43 to 0.95, and for (b) from 0.08 to 0.83 for increasing τ_{ratio}. Other parameter values are $\tau_D = 1$, $\tau_S = 0.5$, $\tau_R = 0.1$, and $G = -1.2$. Frequency range used for the figure corresponds to 0–120 Hz for $\tau_{\text{ON}} = 5$ ms. Note the different scales used.
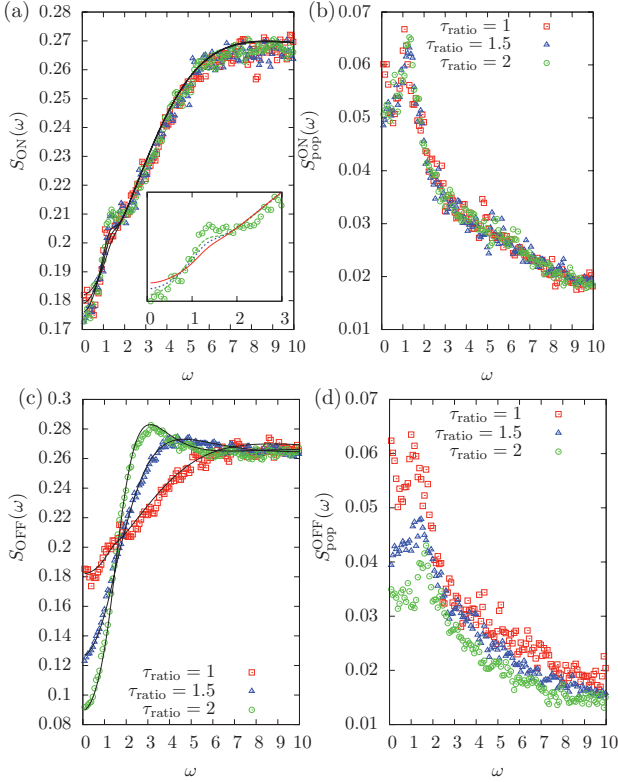
FIG. 8. (Color online) Single-neuron spectra and population spectra for ON (top) and OFF cells (bottom) for $\tau_{\text{ratio}} = 1, 1.5, 2$ and $c = 1$. Other parameters are as in Fig. 2. V_0 has been adjusted so that $r_{\text{ON}} \approx r_{\text{OFF}}$. The effective OFF biases are $\mu_{\text{OFF}} = 0.48, 0.79, 1.001$ for, respectively, $\tau_{\text{ratio}} = 1, 1.5, 2$; the corresponding values for V_0 are $0, 0.305, 0.52$. In panel (a), the LRT curve with the highest bump corresponds to $\tau_{\text{ratio}} = 2$ and the one with the smallest peak to $\tau_{\text{ratio}} = 1$. Inset to panel (a): zoom on the peaks of the LRT curves (solid red, $\tau_{\text{ratio}} = 1$; dotted blue, $\tau_{\text{ratio}} = 1.5$; dashed green, $\tau_{\text{ratio}} = 2$). We also display the numerical results for $\tau_{\text{ratio}} = 2$ for comparison.

With the ratio different from 1, A_{ON} and A_{OFF} [given by Eq. (32)] become different and the feedback may again induce oscillations, provided that the stimulus is spatially correlated [see Eq. (20)]. Figure 8 shows how the single-neuron and population spectra are modified following an increase of τ_{ratio} (the external stimulus is again the Gaussian white noise of unlimited bandwidth). The first thing one may notice is that the ON cells' power spectrum and population spectrum are only slightly modified. The bump at $\omega \approx 1.5$ in the power spectrum [Fig. 8(a)] grows slightly with τ_{ratio}, but reaches nowhere near the one of the ON-only network in Fig. 2(a). In contrast, there is an appreciable effect on the OFF cells' spectral quantities. For $\tau_{\text{ratio}} = 1$, we have the symmetric case showing a small spectral peak at $\omega = 1.5$ [Fig. 8(c), red curve]; with $\tau_{\text{ratio}} = 2$, $\mu_{\text{OFF}} = 1.001$, and the system has just stepped into the deterministic regime, causing the peak around $\omega = 3$. The firing is then dominated by the unperturbed activity of single OFF neurons, and the feedback-induced bump is no longer visible. Remarkably, for $\tau_{\text{ratio}} = 1.5$, for which $\mu_{\text{OFF}} < 1$, we do not see any recovery of the gamma peak. Obviously, this means that the difference between the ON and OFF susceptibilities is not large enough to permit gamma oscillations.
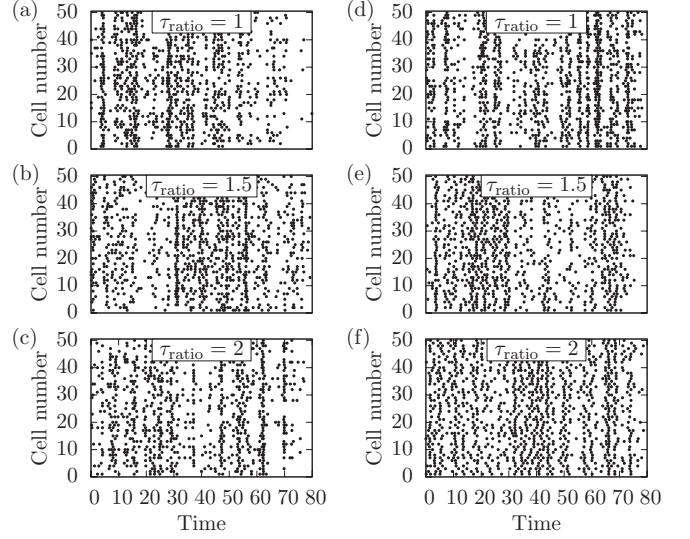

FIG. 9. Raster plots of the activity of ON [(a)–(c)] and OFF [(d)–(f)] cells corresponding to Fig. 8. Notice on the right column [plots (d)–(f)] how the OFF cells' spikings desynchronize with increasing τ_{ratio}.

Figure 8(d) shows that spectral correlations between OFF neurons are impeded when τ_{ratio} is increased. On the other hand, the spectral correlations between ON neurons stay about the same for all values of the ratio [Fig. 8(b)]. This is even more obvious from the raster plots of Fig. 9. Increasing τ_{ratio} uncorrelates the firing of OFF cells and we progressively lose the striped pattern of $\tau_{\text{ratio}} = 1$ [compare Figs. 9(d) and 9(f)]. The OFF cells still oscillate, but in a more independent manner. From Sec. V B, we know that OFF neurons with higher bias and lower internal noise tend to synchronize more in the presence of spatially correlated noise. In the present case, however, their more deterministic behavior is triggered in part by the slower dynamics for $\tau_{\text{ratio}} > 1$ (the other part being due to $V_0 > 0$). This not only affects the intensity of both the internal and external noises—D and D_E become D/τ_{ratio} and D_E/τ_{ratio}, respectively—but also the feedback strength perceived by OFF neurons. With a lower strength G/τ_{ratio}, the feedback is less able to modulate the collective activity of OFF cells. Our results thus indicate that the loss of feedback here dominates over the increased synchrony.

VI. SUMMARY AND CONCLUSION

In this paper, we have derived a LRT for networks containing two classes of neurons, and for which the interactions are predominantly through an all-to-all feedback loop. We obtained expressions for the power spectrum of these cells when submitted to external noise. The primary motivation for this work was the processing done by the ELL of weakly electric fish, in particular, its ability to generate gamma oscillations under spatially correlated stimuli. The ELL contains ON and OFF cells which respond in opposite ways to inputs. We have studied the impact of the OFF cells on the network's oscillatory behavior under stochastic inputs. The model assumed that both the ON and OFF cells send their spike trains to a remote kernel which sums all the incoming spike trains and feeds them back

with a delay to all the cells of the network. When only ON cells are taken into account (ON-only network), this diffuse inhibitory feedback is sufficient to trigger network oscillations when the global input is spatially correlated [13]. We have shown analytically and numerically that including the OFF cells (ON/OFF network) hinders the onset of oscillations for a spatially correlated stimulus.

Neural field theory already showed that gamma oscillations are less prevalent in an ON/OFF network compared to ON-only networks. In that theory, a certain parameter can be computed, R [[14], Eq. (5)], which acts as a global gain parameter that depends on the spatial extent of a spatially homogeneous input. When R exceeds a critical value, oscillations occur. However, this is applicable in the context of deterministic inputs. In the LRT presented here, it is possible to deal with stochastic inputs, and both the feedback strength G and the correlation parameter c explicitly determine the occurrence of an oscillatory state [cf. the expression for the power spectrum Eq. (20)].

Having concluded that bringing the OFF cells into the picture has a negative effect on network oscillations, we then tried to break the symmetry of the ON and OFF cells to see if we can recover the gamma oscillations obtained with an ON-only network [9,13]. In doing so, we had to ensure that the rates of ON and OFF cells are approximately equal to satisfy physiological constraints. The symmetry breakings were also done on the grounds of physiological considerations. First, we increased the bias of OFF cells (through an increase of the offset V_0). This was motivated by their lower spike threshold compared to ON cells. To keep the rates equal, we also decreased the internal noise intensity of OFF cells. The OFF cells were then more deterministic and their spectral cross correlations (as seen on the population spectra) increased with V_0. Such a regularity enhanced the feedback-induced gamma oscillations of the OFF cells [see Figs. 5(b) and 6(b)]. However, the recovered gamma oscillations were far from reaching the same level as that of either the corresponding ON-only network [13] or the experimental results of [9].

Second, we increased the OFF membrane time constant with respect to the ON's. The goal was to mimic the low-pass properties of OFF cells. If the OFF cells are more low pass compared to the ON cells, then it may make room for the latter to oscillate. Again, the constraint of equal firing rates had to be satisfied, and it was achieved by increasing the bias of OFF cells. The cross spectra of ON cells were not modified [Fig. 8(b)] but, contrary to the first asymmetric case, the spectral cross correlations of OFF cells were impeded [Fig. 8(d)]. This was interpreted as a reduction of the synchronization of the OFF cells [and confirmed by the corresponding raster plots, Figs. 9(d)–9(f)]. The power spectra of ON cells showed a slight increase of the height of the feedback-induced peak [Fig. 8(a)]; for the OFF cells, this peak disappears when τ_{ratio} departs from 1 [Fig. 8(c)]. Another peak appears for the OFF cells at higher frequency, which is a direct consequence of the more regular spiking due to the higher effective bias.

Interestingly, both symmetry breakings yielded more regularity in the OFF neurons' firing, but with drastically different results on the collective behavior of the network. On the one hand, the higher bias and the lower intrinsic noise allowed for less random OFF cells' spikings, which consequently helped to synchronize the OFF cells (and to a lesser extent, the ON cells). On the other hand, a slower dynamics for OFF cells, together with a higher bias, strives to reduce the synchronization. Since these symmetry breakings have opposite effects on the feedback-induced gamma oscillations, it seems unlikely that combining them in any way may allow for oscillations as strong as in the ON-only network [13] or the experimental results [9].

Note that, as in [13], we completely ignored the activity of the neurons responsible for the diffuse inhibitory feedback. According to [29], however, this should not invalidate the analysis found in both [13] and in the present paper. Indeed, they show that the dynamics of LIF neurons constituting the feedback kernel have only a marginal effect on the response of the network.

Another point is that both the ON and the OFF cells show gamma oscillations experimentally [7]. Hence, one may wonder why we tried to invoke these oscillations by actually privileging one class of cells with respect to the other. The first reason is that the frequency range for gamma oscillations is large (usually 30–90 Hz). So, it is not excluded that ON and OFF cells show gamma oscillations of different frequencies. Also, as stated in the previous paragraph, even though a combination of the two attempts may not allow one to recover the full strength of gamma oscillations, it may at least bring back some symmetry between the power spectra of ON and OFF cells. Finally, we also believe that the mathematical apparatus derived here may be used in studies of other feedback-driven systems such as the thalamocortical circuit (see, for instance, [30]) or of correlations in recurrent networks [31].

In the end, the simplest hypothesis that preserves the feedback-induced gamma oscillations is that the ON and OFF cells are segregated, i.e., ON cells would be connected (through feedback) only to ON cells and the same for OFF cells. This would be the easiest way to recover the gamma oscillations, but we lack the necessary physiological evidence for such connectivity. Alternatively, future work may require more detailed anatomical and physiological analysis of the ELL feedback circuitry to elucidate the origin of gamma oscillations.

APPENDIX A: PROOF THAT THE ON (OFF) RATE IS A MONOTONICALLY DECREASING (INCREASING) FUNCTION OF V_0

Using Eq. (9), we write

$$
\frac{dr_{\text{ON}}}{dV_0} = \frac{dr_{\text{ON}}}{d\mu_{\text{ON}}}\frac{d\mu_{\text{ON}}}{dV_0} = \frac{dr_{\text{ON}}}{d\mu_{\text{ON}}}\frac{G}{2}\left(\frac{dr_{\text{ON}}}{dV_0} + \frac{dr_{\text{OFF}}}{dV_0}\right),
$$
$$
\frac{dr_{\text{OFF}}}{dV_0} = \frac{dr_{\text{OFF}}}{d\mu_{\text{OFF}}}\left[1 + \frac{G}{2}\left(\frac{dr_{\text{ON}}}{dV_0} + \frac{dr_{\text{OFF}}}{dV_0}\right)\right]. \tag{A1}
$$

Adding the two equations above, isolating $\frac{dr_{\mathrm{ON}}}{dV_0} + \frac{dr_{\mathrm{OFF}}}{dV_0}$ and replacing in Eq. (A1) yields

$$\frac{dr_{\mathrm{ON}}}{dV_0} = \frac{dr_{\mathrm{ON}}}{d\mu_{\mathrm{ON}}} \frac{G}{2} \left[\frac{\frac{dr_{\mathrm{OFF}}}{d\mu_{\mathrm{OFF}}}}{1 - \frac{G}{2}\left(\frac{dr_{\mathrm{ON}}}{d\mu_{\mathrm{ON}}} + \frac{dr_{\mathrm{OFF}}}{d\mu_{\mathrm{OFF}}}\right)} \right],$$

$$\frac{dr_{\mathrm{OFF}}}{dV_0} = \frac{dr_{\mathrm{OFF}}}{d\mu_{\mathrm{OFF}}} \left[1 + \frac{G}{2} \frac{\frac{dr_{\mathrm{OFF}}}{d\mu_{\mathrm{OFF}}}}{1 - \frac{G}{2}\left(\frac{dr_{\mathrm{ON}}}{d\mu_{\mathrm{ON}}} + \frac{dr_{\mathrm{OFF}}}{d\mu_{\mathrm{OFF}}}\right)} \right].$$

As proven in Sec. B 2 of Appendix B, $\frac{dr_{\mathrm{ON}}}{d\mu_{\mathrm{ON}}}$ and $\frac{dr_{\mathrm{OFF}}}{d\mu_{\mathrm{OFF}}}$ are always positive. Since $G < 0$, it is easy to see that $\frac{dr_{\mathrm{ON}}}{dV_0} < 0$. For $\frac{dr_{\mathrm{OFF}}}{dV_0}$, the term in brackets will be positive for

$$2 + |G|\left(\frac{dr_{\mathrm{ON}}}{d\mu_{\mathrm{ON}}} + \frac{dr_{\mathrm{OFF}}}{d\mu_{\mathrm{OFF}}}\right) > |G|\frac{dr_{\mathrm{OFF}}}{d\mu_{\mathrm{OFF}}},$$

which is true for all V_0, hence $\frac{dr_{\mathrm{OFF}}}{dV_0} > 0$.

APPENDIX B: EFFECT OF UNEQUAL MEMBRANE TIME CONSTANTS ON THE LRT

In this appendix, we detail how the dynamics of OFF cells is affected by an increase of their membrane time constant with respect to that of the ON cells. We also delineate its consequences on the analytical results for the rate, the unperturbed spectrum, the susceptibility, and the LRT.

1. Transformation of the OFF cells' dynamics

The unperturbed dynamics of the subthreshold OFF voltage is

$$\tau_{\mathrm{ratio}} \dot{v}_i^{\mathrm{OFF}}(t) = -v_i^{\mathrm{OFF}}(t) + \mu_{\mathrm{OFF}} + \xi_i^{\mathrm{OFF}}(t).$$

Defining $\hat{t} = t/\tau_{\mathrm{ratio}}$ leads to

$$\frac{d\hat{v}_i^{\mathrm{OFF}}}{d\hat{t}}(\hat{t}) = -\hat{v}_i^{\mathrm{OFF}}(\hat{t}) + \mu_{\mathrm{OFF}} + \hat{\xi}_i^{\mathrm{OFF}}(\hat{t}), \qquad \text{(B1)}$$

where we have defined

$$\hat{\xi}_i^{\mathrm{OFF}}(\hat{t}) \equiv \xi_i^{\mathrm{OFF}}(\tau_{\mathrm{ratio}}\hat{t}) \quad \text{and} \quad \hat{v}_i^{\mathrm{OFF}}(\hat{t}) \equiv v_i^{\mathrm{OFF}}(\tau_{\mathrm{ratio}}\hat{t}).$$

The processes $\hat{\xi}_i^{\mathrm{OFF}}(\hat{t})$ obey

$$\left\langle \hat{\xi}_i^{\mathrm{OFF}}(\hat{t})\hat{\xi}_i^{\mathrm{OFF}}(\hat{t}') \right\rangle = 2\hat{D}\delta(\hat{t} - \hat{t}'),$$

with the rescaled noise intensity $\hat{D} = D/\tau_{\mathrm{ratio}}$. Note the important fact that $\mu_{\mathrm{OFF}} = \mu + V_0 + G(r_{\mathrm{ON}} + r_{\mathrm{OFF}})/2$ is invariant with respect to the transformation $t \to t/\tau_{\mathrm{ratio}}$. This is readily seen by considering the transformation of the feedback function $f(t)$. Putting $t = \tau_{\mathrm{ratio}}\hat{t}$ in Eq. (3) gives

$$\hat{f}(\hat{t}) \equiv f(\tau_{\mathrm{ratio}}\hat{t}) = \frac{G}{2N}\int_{\tau_D}^{\infty}\frac{d\tau}{\tau_S}\left(\frac{\tau - \tau_D}{\tau_S}\right)\exp\left(-\frac{\tau - \tau_D}{\tau_S}\right)$$
$$\times \sum_{i=1}^{N}\left[y_i^{\mathrm{ON}}(\tau_{\mathrm{ratio}}\hat{t} - \tau) + y_i^{\mathrm{OFF}}(\tau_{\mathrm{ratio}}\hat{t} - \tau)\right].$$

From the definition of the spike trains, Eq. (4), we have

$$y(\tau_{\mathrm{ratio}}\hat{t}) = \sum_{t_i}\delta(\tau_{\mathrm{ratio}}\hat{t} - t_i)$$
$$= \frac{1}{\tau_{\mathrm{ratio}}}\sum_{\hat{t}_i}\delta(\hat{t} - \hat{t}_i) \equiv \frac{1}{\tau_{\mathrm{ratio}}}\hat{y}(\hat{t}). \qquad \text{(B2)}$$

Here, the $\hat{t}_i$'s are the spike times in units of the OFF membrane time constant and $\hat{y}(\hat{t}) \equiv \sum_{\hat{t}_i}\delta(\hat{t} - \hat{t}_i)$ is the corresponding spike train. We replace this in the expression for the feedback and change variable to $\tau \to \tau/\tau_{\mathrm{ratio}}$ to give

$$\hat{f}(\hat{t}) = \frac{G}{2N}\int_{\tau_D/\tau_{\mathrm{ratio}}}^{\infty}\frac{d\tau}{\tau_S}\left(\frac{\tau\tau_{\mathrm{ratio}} - \tau_D}{\tau_S}\right)\exp\left(-\frac{\tau\tau_{\mathrm{ratio}} - \tau_D}{\tau_S}\right)$$
$$\times \sum_{i=1}^{N}\left[\hat{y}_i^{\mathrm{ON}}(\hat{t} - \tau) + \hat{y}_i^{\mathrm{OFF}}(\hat{t} - \tau)\right].$$

We define $\tau_D = \hat{\tau}_D\tau_{\mathrm{ratio}}$, $\tau_S = \hat{\tau}_S\tau_{\mathrm{ratio}}$, and $G = \hat{G}\tau_{\mathrm{ratio}}$. Doing so, the feedback keeps the same form as before:

$$\hat{f}(\hat{t}) = \frac{\hat{G}}{2N}\int_{\hat{\tau}_D}^{\infty}\frac{d\tau}{\hat{\tau}_S}\left(\frac{\tau - \hat{\tau}_D}{\hat{\tau}_S}\right)\exp\left(-\frac{\tau - \hat{\tau}_D}{\hat{\tau}_S}\right)$$
$$\times \sum_{i=1}^{N}\left[\hat{y}_i^{\mathrm{ON}}(\hat{t} - \tau) + \hat{y}_i^{\mathrm{OFF}}(\hat{t} - \tau)\right].$$

The static part of the feedback is given by

$$\langle\hat{f}\rangle = \frac{\hat{G}}{2}(\hat{r}_{\mathrm{ON}} + \hat{r}_{\mathrm{OFF}}) = \frac{G}{2}(r_{\mathrm{ON}} + r_{\mathrm{OFF}}),$$

where we have transformed the rates measured in units of the ON membrane time constant (u.ON.m.t.c.) to the ones measured in units of the OFF time constant (u.OFF.m.t.c.), i.e., $\hat{r} = \tau_{\mathrm{ratio}}r$. Therefore, it appears that the static part of the feedback is invariant with respect to the transformation $t \to t/\tau_{\mathrm{ratio}}$, and this is the case for the effective bias μ_{OFF} as well.

2. Transformation of the analytical results

When $\tau_{\mathrm{ratio}} > 1$, the formula for the rate of a LIF neuron, Eq. (10), must be replaced by

$$g(\mu, \tau_{\mathrm{ratio}})$$
$$= \left(\tau_R + \tau_{\mathrm{ratio}}\sqrt{\pi}\int_{(\mu-1)/\sqrt{2D/\tau_{\mathrm{ratio}}}}^{\mu/\sqrt{2D/\tau_{\mathrm{ratio}}}}\exp(z^2)\mathrm{erfc}(z)dz\right)^{-1}.$$
$$\text{(B3)}$$

This equation is obtained by replacing $D \to \hat{D}$ and $\tau_R \to \hat{\tau}_R = \tau_R/\tau_{\mathrm{ratio}}$ in Eq. (10), and by using the conversion between rates measured in different units. Note that for Gaussian white noise stimuli of unlimited bandwidth, we would use $Q = D + D_E$ as the noise intensity. We now want to prove that r_{OFF} decreases with τ_{ratio}, i.e., that $\frac{dr_{\mathrm{OFF}}}{d\tau_{\mathrm{ratio}}} < 0$. In what follows we keep V_0 fixed. The rates are obtained by solving the following coupled equations in a self-consistent way [compare with Eq. (11)]:

$$r_{\mathrm{ON}} = \nu[\mu_{\mathrm{ON}}(\tau_{\mathrm{ratio}})] \quad \text{and} \quad r_{\mathrm{OFF}} = g[\mu_{\mathrm{OFF}}(\tau_{\mathrm{ratio}}), \tau_{\mathrm{ratio}}]$$

with ν given by Eq. (10) and g given by Eq. (B3) above. Note that both rates are expressed in u.ON.m.t.c. and that only

$g(\mu_{\text{OFF}}, \tau_{\text{ratio}})$ explicitly depends on τ_{ratio}. The derivatives of the rates with respect to τ_{ratio} are

$$\frac{dr_{\text{ON}}}{d\tau_{\text{ratio}}} = \frac{dr_{\text{ON}}}{d\mu_{\text{ON}}} \frac{d\mu_{\text{ON}}}{d\tau_{\text{ratio}}} = \frac{G}{2} \frac{dr_{\text{ON}}}{d\mu_{\text{ON}}} \left(\frac{dr_{\text{ON}}}{d\tau_{\text{ratio}}} + \frac{dr_{\text{OFF}}}{d\tau_{\text{ratio}}} \right),$$

$$\frac{dr_{\text{OFF}}}{d\tau_{\text{ratio}}} = \frac{G}{2} \frac{dr_{\text{OFF}}}{d\mu_{\text{OFF}}} \left(\frac{dr_{\text{ON}}}{d\tau_{\text{ratio}}} + \frac{dr_{\text{OFF}}}{d\tau_{\text{ratio}}} \right) + \frac{\partial r_{\text{OFF}}}{\partial \tau_{\text{ratio}}}.$$

Adding them together and isolating ($\frac{dr_{\text{ON}}}{d\tau_{\text{ratio}}} + \frac{dr_{\text{OFF}}}{d\tau_{\text{ratio}}}$) yields

$$\left(\frac{dr_{\text{ON}}}{d\tau_{\text{ratio}}} + \frac{dr_{\text{OFF}}}{d\tau_{\text{ratio}}} \right) = \frac{\frac{\partial r_{\text{OFF}}}{\partial \tau_{\text{ratio}}}}{1 - \frac{G}{2} \left(\frac{dr_{\text{ON}}}{d\mu_{\text{ON}}} + \frac{dr_{\text{OFF}}}{d\mu_{\text{OFF}}} \right)}.$$

Hence,

$$\frac{dr_{\text{OFF}}}{d\tau_{\text{ratio}}} = \frac{\partial r_{\text{OFF}}}{\partial \tau_{\text{ratio}}} \left[\frac{\frac{dr_{\text{OFF}}}{d\mu_{\text{OFF}}}}{1 - \frac{G}{2} \left(\frac{dr_{\text{ON}}}{d\mu_{\text{ON}}} + \frac{dr_{\text{OFF}}}{d\mu_{\text{OFF}}} \right)} + 1 \right]. \quad \text{(B4)}$$

Let us define

$$\frac{\mu_{\text{OFF}}}{\sqrt{2D/\tau_{\text{ratio}}}} \equiv b, \quad \frac{\mu_{\text{OFF}} - 1}{\sqrt{2D/\tau_{\text{ratio}}}} \equiv a$$

with $b = a + \sqrt{\frac{\tau_{\text{ratio}}}{2D}} > a$. On the one hand, we have

$$\frac{\partial r_{\text{OFF}}}{\partial \tau_{\text{ratio}}} = -r_{\text{OFF}}^2 \sqrt{\pi} \left\{ \int_a^b \exp(z^2) \text{erfc}(z) dz \right.$$
$$\left. + \frac{b}{2} \exp(b^2) \text{erfc}(b) - \frac{a}{2} \exp(a)^2 \text{erfc}(a) \right\},$$

which is smaller than zero because the function $h(x) = x \exp(x^2) \text{erfc}(x)$ is strictly increasing and the first term between the accolades is positive. On the other hand,

$$\frac{dr_{\text{ON}}}{d\mu_{\text{ON}}} = \sqrt{\frac{\pi}{2D}} r_{\text{ON}}^2 \left[\exp\left(\frac{a^2}{\tau_{\text{ratio}}} \right) \text{erfc}\left(\frac{a}{\sqrt{\tau_{\text{ratio}}}} \right) \right.$$
$$\left. - \exp\left(\frac{b^2}{\tau_{\text{ratio}}} \right) \text{erfc}\left(\frac{b}{\sqrt{\tau_{\text{ratio}}}} \right) \right]$$

and

$$\frac{dr_{\text{OFF}}}{d\mu_{\text{OFF}}} = \sqrt{\frac{\tau_{\text{ratio}}^3 \pi}{2D}} r_{\text{OFF}}^2 [\exp(a^2) \text{erfc}(a) - \exp(b^2) \text{erfc}(b)]$$

are always positive since $\exp(x^2) \text{erfc}(x)$ is monotonically decreasing. Therefore, the term in square brackets in Eq. (B4) is always positive and r_{OFF} decreases with τ_{ratio}.

The unperturbed power spectrum for OFF neurons in u.OFF.m.t.c., $\hat{S}^{(0)}(\hat{\omega}, \mu_{\text{OFF}}, \hat{D}) \equiv \hat{S}_{\text{OFF}}^{(0)}(\hat{\omega})$, is obtained from Eq. (12)—without the term proportional to $\delta(\omega)$—by replacing the parameters and variables by their hatted counterparts. Note in this respect that $\hat{\Delta}_{\text{OFF}}$ and $\hat{\omega}$ are linked to the corresponding quantities in u.ON.m.t.c. by

$$\hat{\Delta}_{\text{OFF}} = \tau_{\text{ratio}} \Delta_{\text{OFF}} \quad \text{and} \quad \hat{\omega} = \tau_{\text{ratio}} \omega. \quad \text{(B5)}$$

It is useful for graphing and computation purposes to have the OFF power spectrum in u.ON.m.t.c.. One can show that this is obtained from the spectrum in u.OFF.m.t.c. by replacing $\hat{\omega} = \tau_{\text{ratio}} \omega$ and dividing by τ_{ratio}:

$$S_{\text{OFF}}(\omega) = \frac{1}{\tau_{\text{ratio}}} \hat{S}_{\text{OFF}}(\tau_{\text{ratio}} \omega).$$

The intuitive rationale behind the prefactor $1/\tau_{\text{ratio}}$ is that the power spectrum is measured in Hz when the second is the unit of time. Therefore, changing the way we count time changes the scaling factor of the power spectrum too. Using the same intuitive argumentation, we have for the OFF susceptibility

$$A_{\text{OFF}}(\omega) = \frac{1}{\tau_{\text{ratio}}} \hat{A}_{\text{OFF}}(\tau_{\text{ratio}} \omega). \quad \text{(B6)}$$

This follows at once from the facts that D_E has dimension [time] when the voltage is dimensionless and time is measured in seconds, and that $2D_E |A|^2$, the first order response to noise, must have dimension $[\text{time}]^{-1}$.

Gathering all these results leads to the unperturbed power spectrum of the OFF cells in u.ON.m.t.c.:

$$S_{\text{OFF}}^{(0)} = r_{\text{OFF}} \frac{\left| \mathcal{D}_{i \tau_{\text{ratio}} \omega} \left(\frac{\mu_{\text{OFF}} - v_T}{\sqrt{\hat{D}}} \right) \right|^2 - e^{2\tau_{\text{ratio}} \Delta_{\text{OFF}}} \left| \mathcal{D}_{i \tau_{\text{ratio}} \omega} \left(\frac{\mu_{\text{OFF}} - v_R}{\sqrt{\hat{D}}} \right) \right|^2}{\left| \mathcal{D}_{i \tau_{\text{ratio}} \omega} \left(\frac{\mu_{\text{OFF}} - v_T}{\sqrt{\hat{D}}} \right) - e^{\tau_{\text{ratio}} \Delta_{\text{OFF}}} e^{i\omega \tau_R} \mathcal{D}_{i \tau_{\text{ratio}} \omega} \left(\frac{\mu_{\text{OFF}} - v_R}{\sqrt{\hat{D}}} \right) \right|^2} \quad \text{(B7)}$$

and to the OFF susceptibility (in u.ON.m.t.c.)

$$A_{\text{OFF}} = \tau_{\text{ratio}} \left(\frac{i\omega r_{\text{OFF}}}{\sqrt{\hat{D}} (i \tau_{\text{ratio}} \omega - 1)} \right)$$
$$\times \frac{\mathcal{D}_{i \tau_{\text{ratio}} \omega - 1} \left(\frac{\mu_{\text{OFF}} - v_T}{\sqrt{\hat{D}}} \right) - e^{\tau_{\text{ratio}} \Delta_{\text{OFF}}} \mathcal{D}_{i \tau_{\text{ratio}} \omega - 1} \left(\frac{\mu_{\text{OFF}} - v_R}{\sqrt{\hat{D}}} \right)}{\mathcal{D}_{i \tau_{\text{ratio}} \omega} \left(\frac{\mu_{\text{OFF}} - v_T}{\sqrt{\hat{D}}} \right) - e^{\tau_{\text{ratio}} \Delta_{\text{OFF}}} e^{i\omega \tau_R} \mathcal{D}_{i \tau_{\text{ratio}} \omega} \left(\frac{\mu_{\text{OFF}} - v_R}{\sqrt{\hat{D}}} \right)}. \quad \text{(B8)}$$

3. Transformation of the LRT

The perturbed time evolution for the OFF cells is now given by

$$\frac{d\hat{v}_i^{\text{OFF}}}{d\hat{t}}(\hat{t}) = -\hat{v}_i^{\text{OFF}}(\hat{t}) + \mu_{\text{OFF}} + \hat{\xi}_i^{\text{OFF}}(\hat{t}) + \hat{f}(\hat{t})$$
$$- \langle \hat{f}(\hat{t}) \rangle - \hat{\zeta}_i(\hat{t}).$$

This equation produces spike trains $\hat{y}_i^{\text{OFF}}(\hat{t})$ in u.OFF.m.t.c. The LRT equation for the OFF cells corresponding to Eq. (15) is ($\epsilon = -1$ and the tilde denotes the Fourier transform)

$$\tilde{\hat{y}}_i^{\text{OFF}}(\hat{\omega}) = \tilde{\hat{y}}_{\text{OFF},i}^{(0)}(\hat{\omega}) + \hat{A}(\hat{\omega}, \mu_{\text{OFF}}, \hat{D})$$
$$\times \left[-\tilde{\hat{\zeta}}_i(\hat{\omega}) + \frac{\hat{F}(\hat{\omega})}{2N} \left(\sum_{k=1}^N \tilde{\hat{y}}_k^{\text{ON}}(\hat{\omega}) + \sum_{k=1}^N \tilde{\hat{y}}_k^{\text{OFF}}(\hat{\omega}) \right) \right]$$

with

$$\hat{F}(\hat{\omega}) = \hat{G} \frac{e^{i\hat{\omega}\hat{\tau}_D}}{(1 - i\hat{\omega}\hat{\tau}_S)^2} = \frac{G}{\tau_{\text{ratio}}} \frac{e^{i\omega\tau_D}}{(1 - i\omega\tau_S)^2}$$

$$= \frac{1}{\tau_{\text{ratio}}} F(\omega)$$

and

$$\tilde{y}_i^{\text{OFF}}(\hat{\omega}) \equiv \int_0^{T/\tau_{\text{ratio}}} \hat{y}_i^{\text{OFF}}(\hat{t}) e^{i\hat{\omega}\hat{t}} \, d\hat{t}$$

$$= \frac{1}{\tau_{\text{ratio}}} \int_0^T \hat{y}_i^{\text{OFF}}(t/\tau_{\text{ratio}}) e^{i\omega t} \, dt = \tilde{y}_i^{\text{OFF}}(\omega),$$

because of Eq. (B2). For $\tilde{\hat{\zeta}}_i(\hat{\omega}) = \sqrt{c}\tilde{\hat{\eta}}_c(\hat{\omega}) + \sqrt{1-c}\tilde{\hat{\eta}}_i(\hat{\omega})$, we have

$$\tilde{\hat{\zeta}}_i(\hat{\omega}) = \int_0^{T/\tau_{\text{ratio}}} \hat{\zeta}_i(\hat{t}) e^{i\hat{\omega}\hat{t}} \, d\hat{t}$$

$$= \frac{1}{\tau_{\text{ratio}}} \int_0^T \hat{\zeta}_i(t/\tau_{\text{ratio}}) e^{i\omega t} \, dt = \frac{1}{\tau_{\text{ratio}}} \int_0^T \zeta_i(t) e^{i\omega t} \, dt,$$

so that

$$\tilde{\hat{\zeta}}_i(\hat{\omega}) = \tilde{\zeta}_i(\omega)/\tau_{\text{ratio}}. \tag{B9}$$

In the end, Eqs. (18) remain unchanged except for the replacement of the A_{OFF} of Eq. (13) by the one given by Eq. (B8). The accuracy of this transformed LRT can be seen in Figs. 8(a) and 8(c).

---

[1] G. Buzsàki and A. Draguhn, Science **304**, 1926 (2004).

[2] G. Buzsàki, *Rhythms of the Brain* (Oxford University Press, Oxford, NY, 2006).

[3] X.-J. Wang, Physiol. Rev. **90**, 1195 (2010).

[4] G. Buzsàki and X.-J. Wang, Annu. Rev. Neurosci. **35**, 203 (2012).

[5] H. Spekreijse and H. Oosting, Kybernetik **7**, 22 (1970).

[6] L. Maler, in *Computational Neuroscience: Theoretical Insights into Brain Function*, edited by T. D. Paul Cisek and J. F. Kalaska, Progress in Brain Research, Vol. 165 (Elsevier, Amsterdam, 2007), pp. 135–154.

[7] B. Doiron, M. J. Chacron, L. Maler, A. Longtin, and J. Bastian, Nature (London) **421**, 539 (2003).

[8] M. J. Chacron, B. Doiron, L. Maler, A. Longtin, and J. Bastian, Nature (London) **423**, 77 (2003).

[9] B. Doiron, B. Lindner, A. Longtin, L. Maler, and J. Bastian, Phys. Rev. Lett. **93**, 048101 (2004).

[10] L. Maler, J. Comp. Neurol. **183**, 323 (1979).

[11] N. J. Berman and L. Maler, J. Exp. Biol. **202**, 1243 (1999).

[12] M. J. Chacron, A. Longtin, and L. Maler, Phys. Rev. E **72**, 051917 (2005).

[13] B. Lindner, B. Doiron, and A. Longtin, Phys. Rev. E **72**, 061919 (2005).

[14] J. Lefebvre, A. Longtin, and V. G. LeBlanc, Phys. Rev. E **80**, 041912 (2009).

[15] J. Lefebvre, A. Longtin, and V. LeBlanc, J. Biol. Phys. **37**, 189 (2011).

[16] R. Krahe, J. Bastian, and M. J. Chacron, J. Neurophysiol. **100**, 852 (2008).

[17] G. Kreiman, R. Krahe, W. Metzner, C. Koch, and F. Gabbiani, J. Neurophysiol. **84**, 189 (2000).

[18] J. de la Rocha, B. Doiron, E. Shea-Brown, K. Josić, and A. Reyes, Nature (London) **448**, 802 (2007).

[19] E. Shea-Brown, K. Josić, J. de la Rocha, and B. Doiron, Phys. Rev. Lett. **100**, 108102 (2008).

[20] B. Lindner, L. Schimansky-Geier, and A. Longtin, Phys. Rev. E **66**, 031916 (2002).

[21] B. Lindner, Ph.D. thesis, Humboldt-Universität zu Berlin, 2002.

[22] O. Ávila Åkerberg and M. J. Chacron, Phys. Rev. E **79**, 011914 (2009).

[23] O. Ávila Åkerberg and M. J. Chacron, Math. Modell. Nat. Phenom. **5**, 100 (2010).

[24] B. Lindner, M. J. Chacron, and A. Longtin, Phys. Rev. E **72**, 021911 (2005).

[25] We consider $\omega \neq 0$ to avoid the cumbersome δ functions that appear in the process.

[26] W. H. Mehaffey, L. Maler, and R. W. Turner, J. Neurophysiol. **99**, 2641 (2008).

[27] L. D. Ellis, W. H. Mehaffey, E. Harvey-Girard, R. W. Turner, L. Maler, and R. J. Dunn, J. Neurosci. **27**, 9491 (2007).

[28] A. Borst and F. E. Theunissen, Nat. Neurosci. **2**, 947 (1999).

[29] D. Marinazzo, H. J. Kappen, and S. C. A. M. Gielen, Neural Comput. **19**, 1739 (2007).

[30] A. M. Sillito, H. E. Jones, G. L. Gerstein, and D. C. West, Nature (London) **369**, 479 (1994).

[31] J. W. Pillow, J. Shlens, L. Paninski, A. Sher, A. M. Litke, E. J. Chichilnisky, and E. P. Simoncelli, Nature (London) **454**, 995 (2008).